

Liquid jet in swirling cross flows- A numerical investigation

Surya Prakash, Suhas S Jain*, Raghunandan B. N., Ravikrishna R. V. *, Gaurav Tomar*

Abstract— Liquid jet in cross flow finds direct applications in different engineering fields, more specifically in the aerospace industry and gas turbine engines. This article presents Volume-Of-Fluid based numerical simulations of a liquid jet injected into gas cross flow in swirling motion. The liquid jet is injected radially outwards from a central tube to a confined annular space with gas cross flow – a configuration that may be found in modern gas turbine combustors. The simulations are conducted at high liquid-to-gas density ratio (D) of 180:1 and liquid-to-gas momentum ratio (Q) of 20. The Swirl Number (SN) of the gas cross flow is varied between 0 and 0.84. The liquid jet undergoes column and shear modes of breakup as observed in experimental studies. The fluctuations in spray trajectory are also captured that are caused by the variations in column breakup lengths which in turn give rise to a whiplash action of the liquid jet. The trajectory of the spray is analysed in terms of radial penetration and angular deflection. The radial penetration is observed to follow the well-established power-law, depending primarily on momentum ratio and angular deflection is observed to vary directly proportional to Swirl Numbers. The drop size measurements are made at different locations downstream up to 35 diameters. A simple criterion based on the shape of the droplet is defined as a better and more practical alternative to the regular Sphericity number. Only those droplets falling below a set threshold are considered for further analyses. It is observed that the drop-size distribution closely follows the log-normal distribution. The Sauter Mean Diameter (SMD) of the droplets are found to increase along the streamwise direction, which is attributed to the phenomenon of coalescence of droplets. It may be stated that these high-fidelity numerical simulations successfully capture the physics involved in the breakup of a liquid jet in cross flow – most important being that of primary breakup.

Index Terms— Spray, cross flow, primary atomization, numerical simulation, VOF, drop size distribution, trajectory.

I. INTRODUCTION

Liquid jet in cross flow (LJICF) finds application in combustors of gas turbine engines. There has been a renewed interest in this field over the past decade borne out of requirements to reduce pollutant emissions and fuel costs. This can be achieved by increasing the efficiency of combustion which requires more effective fuel injection systems. Though

many experimental studies [2,3,20] have been conducted on this topic, most of them deal with atmospheric conditions. This is an understandable limitation due to the complexities involved in setting up the experiments under elevated pressures and temperatures. This is where the numerical investigation can aid in better understanding of the involved physics. The non-dimensional parameters that are widely believed to characterise the behaviour of LJICF [2] are the Aerodynamic Weber number (We) and the liquid-to-gas momentum flux ratio (Q) and Swirl Number (SN) in the presence of swirling flows.

The jet penetration, spray trajectory, drop size and mass flux distributions have all been reported to vary with We and Q . Different stages of break up have been identified and a breakup regime map has been developed [3]. Multimode breakup exhibits column breakup, bag breakup, ligament breakup and shear breakup of the liquid jet at different locations. Multiple complex processes of break up occur simultaneously and the resultant dense spray limits the ability of experimental investigation. Simulation of such a multiphase flow poses a challenge in itself due to the complexities involved in the flow and interaction between the two fluids. In general, the liquid-air flows are characterised by high-density ratio, high surface tension values and low viscosities. The process of atomization of the liquid jet due to cross flow resulting in fine droplets also introduces a wide range of spatial scales into the problem. The prominent interface tracking methods namely the Volume-of-Fluid (VOF), the Level-set and the Front-tracking methods have been implemented to simulate liquid gas interaction flows [4–6]. Tomar et al. [7] have used the VOF scheme to study the atomization of liquid jet with a co-axial flow of air. They introduced a multiscale model with Eulerian-Lagrangian two-way coupling method to efficiently compute the physics involved at different spatial scales. In this approach, the particles are modelled separately on which Lagrangian advection is performed and the continuous phase is solved using Finite Volume method. The well-known jet atomization process involves the primary breakup where the jet is disintegrated into ligaments and the secondary breakup where these ligaments disintegrate further into spherical droplets. The fine droplets formed at the end of these processes continue to remain intact without undergoing further breakup.

Hermann [8] and Kim [9] et al. have utilised the multiscale modelling to simulate liquid jet breakup, with a modified Level-set method for interface tracking. Hermann [10] has

Surya Prakash R. and Prof. B. N. Raghunandan are with the Department of Aerospace Engineering, Indian Institute of Science, Bangalore, India.

Suhas S Jain, Prof. R. V. Ravikrishna and Dr. Gaurav Tomar are with the Department of Mechanical Engineering, Indian Institute of Science, Bangalore, India..

utilised their balanced force refined level set grid (RLSG) method to simulate the injection of liquid into cross flow. They reported results to be mostly matching those of experimental studies in terms of jet penetration and resultant drop sizes. Though the simulations matched the non-dimensional parameters, the density-ratio had to be artificially kept low due to the limitations of numerical schemes. In a recent study, Hermann [11] showed that higher density ratio results in increased penetration and decreased jet core deformation in the transverse direction.

The current numerical investigation focuses upon the breakup of a liquid jet in cross flow at simulated elevated pressures of 5 bars corresponding to a density ratio of 180:1. An annular geometry is used to enable the study of the effects of swirling gas flow. The following sections present the results thus obtained from these simulations and discuss the analysis of spray trajectory and drop size distributions.

II. NUMERICAL METHODS

An open source code Gerris [7,15,16] has been used for the simulations presented in this study. In the following, we present a brief discussion on the numerical scheme employed in Gerris for the two-phase flow simulations. The modified Navier–Stokes equation representing the incompressible two-phase flow with implicit interface boundary conditions [12] is given as

$$\rho[\delta t u + (u \cdot \nabla)u] = -\nabla p + \nabla \cdot (2\mu D) + \sigma \kappa \delta s n$$

where $u = (u, v, w)$ is the fluid velocity, $\rho \equiv \rho(x, t)$ is the fluid density, $\mu \equiv \mu(x, t)$ is the dynamic viscosity and D , the deformation tensor, is defined as $D_{ij} \equiv (\delta_i u_j + \delta_j u_i)/2$. The surface tension force is non-zero only at the interface as signified by the Dirac delta function, δs , with σ , n and κ representing the surface-tension coefficient, the unit normal and the curvature at the interface, respectively.

The advection equation for density and the incompressibility condition are given by

$$\begin{aligned} \delta t \rho + \nabla \cdot (\rho u) &= 0, \\ \nabla \cdot u &= 0 \end{aligned}$$

The density and the viscosity field are obtained using a linear interpolation based on the void-fraction field:

$$\begin{aligned} \rho(c) &\equiv c\rho_1 + (1-c)\rho_2, \\ \mu(c) &\equiv c\mu_1 + (1-c)\mu_2 \end{aligned}$$

The methodology adopted for solving the two-phase, sharp interface, incompressible flow equations are presented in detail in [15–17]. In what follows, we briefly mention the essential steps of the algorithm.

The cell-centered auxiliary velocity field is calculated by excluding the pressure gradient in the Navier–Stokes equation. The face centred velocities are then obtained by averaging the cell centred values on all the faces. The pressure field is calculated to obtain a divergence-free velocity field and the face-centered velocities are corrected and are used to compute the cell-centered velocities. The volume fraction is advected using this velocity field [18] using a second order operator splitting algorithm. Balanced-force surface-tension calculation [19] is then used to calculate the surface tension forces. An

oortree-based adaptive mesh refinement is used based on criteria like vorticity, the gradient of a variable [15] or the curvature of the interface [16]. This is carried out very efficiently costing not more than 1 per-cent of the computation time

III. RESULTS AND DISCUSSION

All the governing parameters are calculated in terms of non-dimensional numbers, namely, aerodynamic Weber number (We), Liquid-to-gas momentum ratio (Q) and Swirl number (SN) of the gas flow. Numerical investigations are carried out for momentum ratios of 20 and 25 and swirl numbers 0, 0.42 and 0.84. The computational domain is an annular region with the ratio of inner to outer radii kept at 2:5 as shown in Fig. 1. Ideal analytical velocity profiles (solid body rotation) are utilised at the inlet to obtain the swirling flow in the annular space. The simulation conditions are tabulated in Table 1. The diameter of the liquid injector may be equivalently considered as 1-mm for quantification purposes. The liquid jet is injected radially outwards from the inner annular tube having a plug velocity profile simulating that of a nozzle with very short L/d ratio.

It becomes imperative for a spray formed in confinement that it does not impinge on the outer walls. Excess penetration will result in the formation of a liquid film on the upper surface and hinders the process of obtaining the trajectory information. The conditions in the present simulation are chosen so as to keep the spray clear of the outer walls. The drops that impinge the wall stick/splash.

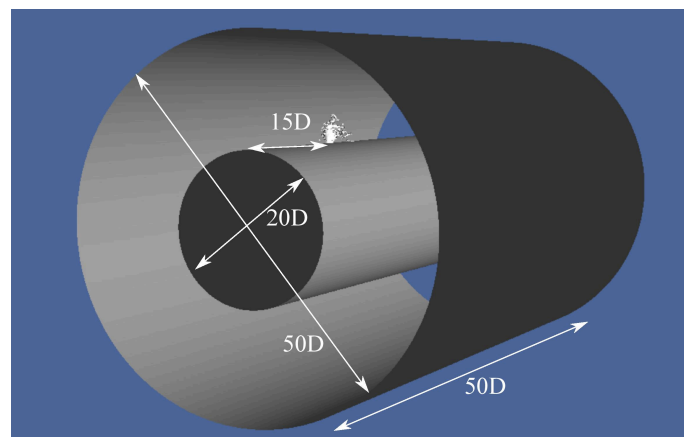


Fig. 1. The computational domain used for liquid jet in swirling cross flow simulations – showing a 3-D representation and a 2-D cross section of the same. Note that the mesh is adaptively refined in favour of the liquid phase.

The maximum refinement of the computational domain corresponds to a spatial resolution of 24 microns which we believe is good enough to capture the fine droplets produced during breakup. The breakup of the jet is captured being very similar to that found in experimental studies. The liquid jet manifests all the features that are observed during a liquid jet breakup in cross flow – the instabilities formed on the windward side of the jet, the column breakup features and the

tendency to form bag-like structures – which may be seen clearly in Fig. 2 and also in Figs. 3a and 3b.

Figure 3a shows the liquid jet breakup for $Q=20$ and $SN = 0$ whereas Figure 3b shows the breakup for $SN=0.42$. It may be noted here that the momentum ratio is calculated purely based on the axial component of the velocity in the computational domain. The liquid jet in the swirling case effectively experiences a higher total velocity and as a consequence exhibits faster breakup. The trajectories and the resultant drop size distributions are analysed in the following sections.

Table 1 Vital parameters and conditions used for simulations

Liquid-to-gas momentum ratio (Q)	20,25
Swirl Numbers (SN)	0, 0.42 and 0.84
Liquid-to-gas density ratio (D)	180
Computational domain length	50 diameters (Injector at $15d$ from entrance)
Annular space height	15 diameters

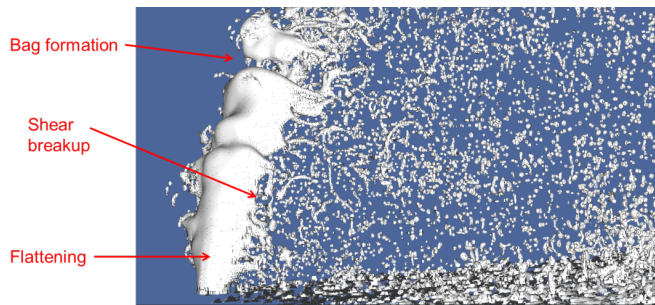
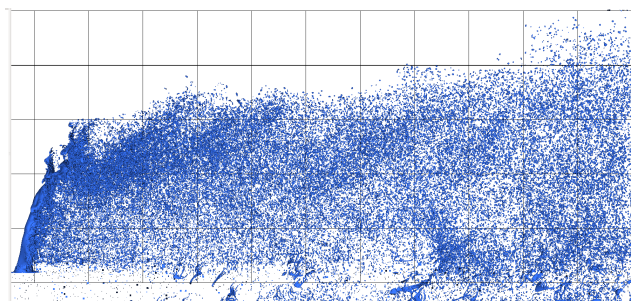
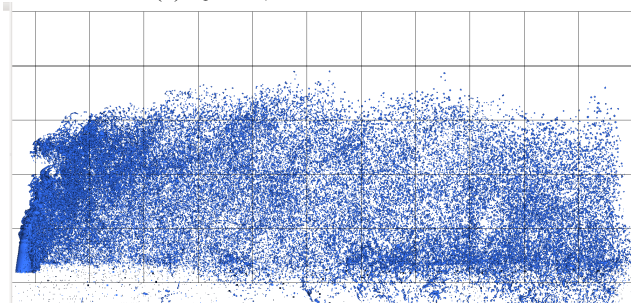


Fig. 2 Liquid jet breakup showing all the primary atomization features.



(a) $Q = 20$; $SN = 0$: Front View



(b) $Q = 20$; $SN = 0.42$: Front View

Fig. 3. Front view of the resultant spray formed from the liquid jet in cross flow at different conditions

A. Trajectory

The trajectory of a liquid jet in cross flow forms a vital design parameter for the construction of a gas turbine engine. Thus, the trajectories of the jets are quantified for both the swirling and the non-swirling cases. It was proposed by Wu et al. [3] that the trajectory of a resultant spray may be given by the correlation:

$$r = 0.55 Q^{0.5} x^{0.5}$$

where the distances r and x are normalised by the jet diameter. This has been agreed upon by the subsequent experimental studies as well. Though there have been a few revisions to this expression, the essential form remains the same with minor modifications to the constants involved. It may be observed that the trajectory is directly dependent on the liquid-to-gas momentum ratio only and not on the Aerodynamic Weber number. Therefore, while the Aerodynamic Weber number dictates the transitions between the regimes of breakup the liquid-to-gas momentum ratio influences the trajectory of the spray. It may also be noted here that while the trajectories may be derived to represent either the centre line or the outer windward boundary of the spray, the current study uses the latter.

The simulation is run for 4-5 flow pass-throughs by which time the spray has been observed to have reached a quasi-steady state after the initial disturbances caused by the issuance of the liquid jet tip into the cross flow environment. The steady state is established in terms of the number of droplets passing through any given cross section of the computational domain for a small period of time. This is found to reach the quasi-steady state with some periodical variations occurring due to the familiar whiplash action of the jet, which has been consistently reported even by the experimental studies. At this quasi-steady state, there are around 4000+/-500 droplets passing through any cross-section of thickness $2.5d$.

In the annular configuration, the spray traverses a three-dimensional path which implies that a single expression does not suffice to paint the complete picture of the trajectory. Therefore, the trajectory is hereby expressed in terms of both the radial penetration - r and the angular deflection θ . Figure 4 shows the schematic for the coordinates used for the calculation of the trajectory. The trajectory is then calculated during the quasi-steady state and time-averaging the data to account for the crests and troughs formed on the outer windward boundary of the jet.

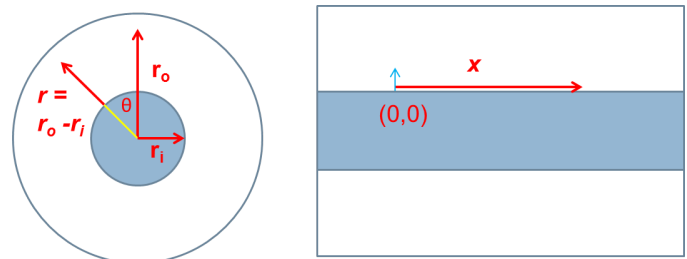


Fig. 4. Representative coordinates utilised for calculation of trajectory (Not to scale)

Thus, the expressions used to capture the trajectory are:

$$r = a Q^{0.5} x^c \text{ and } \theta = f(SN, x)$$

The exponent of momentum ratio, Q is assumed to be 0.5 taking a cue from the already established expressions available in the literature, though not involving swirling flows. The expression for angular deflection is to be derived based on the observations.

Figure 5 shows the trajectories for $SN = 0, 0.42$ and 0.84 . The numerical data obtained is also curve-fitted with the correlation representing the above expression. It may be observed that the simulation data and the corresponding correlated curves match satisfactorily.

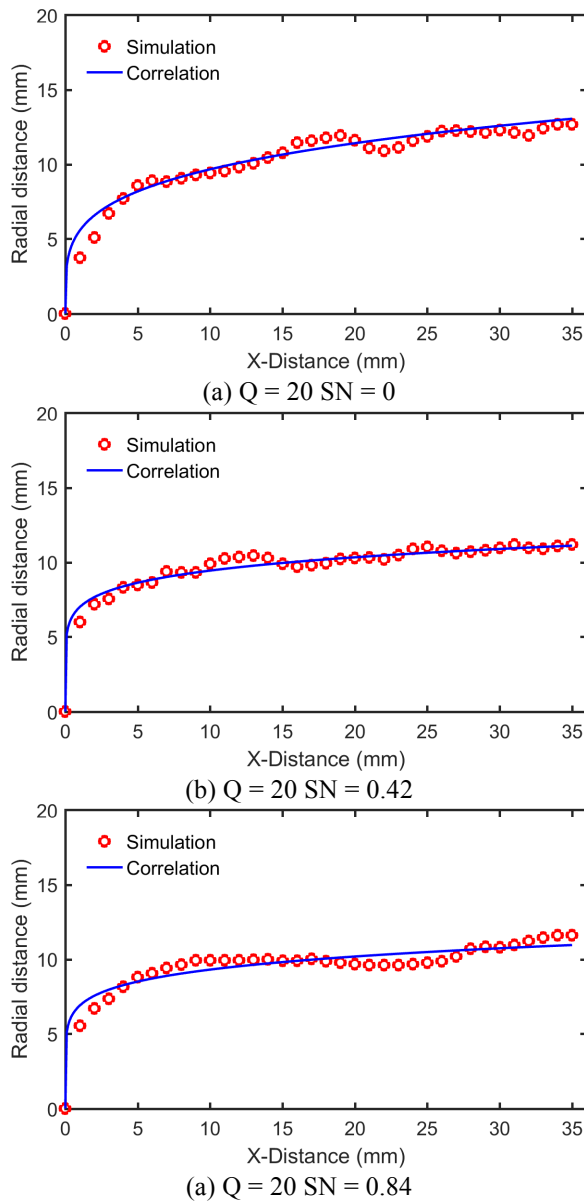


Fig. 5. Radial penetration of the spray in swirling cross flows for $Q = 20$; $SN = 0, 0.42$ and 0.84 respectively

The swirl cases are also analysed for the angular deflection of the spray and a correlation for its variation is derived. Figure 6 shows the variation of spray angular deflection with

axial distance. It may be observed that the angle of deflection varies linearly with axial distance and their slopes are proportional to the corresponding swirl numbers. The values of b, c and k for the best fits are calculated and the resultant expressions for radial penetration and angular deflection are given as:

$$r = 1.27 Q^{0.5} x^{0.21} \text{ and } \theta = 2 SN x$$

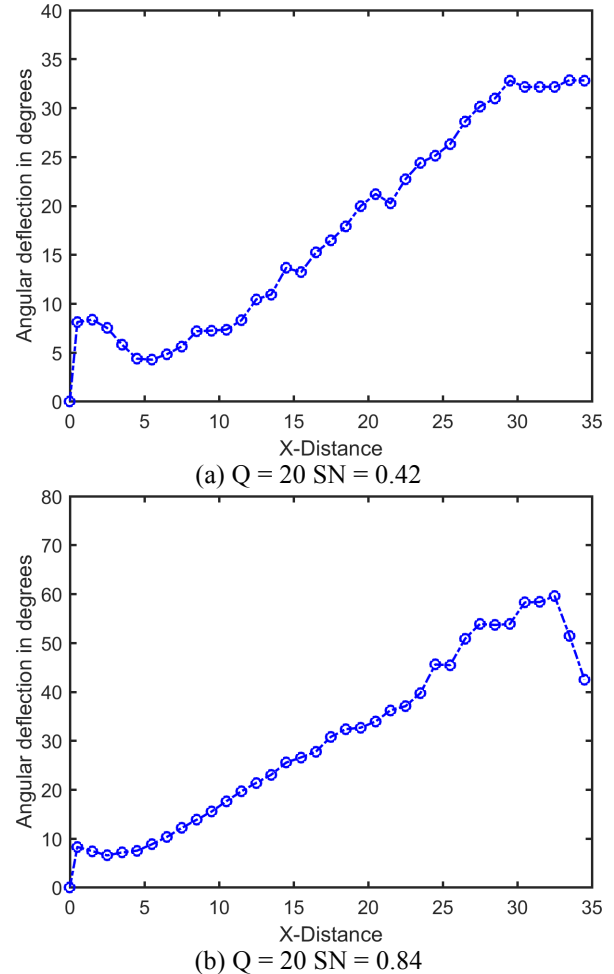


Fig. 6. Angular deflection of the spray in swirling cross flows for $SN = 0.42$ and 0.84 respectively

B. Drop size distribution

The drop size distribution of the resultant spray is analysed and presented in this section. The liquid jet undergoes columns breakup, shear breakup and breakup through bag-like structures. While these mechanisms form the primary atomization part of the liquid jet breakup, the larger drops and ligaments undergo further breakup into smaller droplets completing the breakup through secondary atomization. The variation of drop size distribution in the streamwise direction is analysed and is found that a stable state is reached at around 30 diameters downstream of the location of injection. Another important criterion –Shape factor - is defined as the ratio of the largest radius to the mean radius of the liquid drop, to characterise the shape of the droplets formed. This is an alternative to the conventionally used definition of sphericity and gives a wider range of derived numbers to effectively

classify ligaments and near-spherical droplets. All the droplets that have not impinged on the inner tube and are below the threshold of shape factor of 3 are included in the drop size analysis.

Figures 7 and 8 show the drop size distributions at various downstream locations. It is observed that the drop sizes obtained after the jet breakup follow the Log-normal distribution closer than other distributions. This observation is found to be consistent at all locations for both the swirling and the non-swirling case. Table 2 lists the summary of drop-sizing results obtained for all the cases under investigation. It is found that the Sauter mean Diameter of the drops increases

in magnitude as we move downstream until the exit. This behaviour is attributed to the coalescence of drops happening all along the flow within the domain under current study. Both the drop-size-distributions as well as the SMD numbers are found to be well within the range of those found in experimental studies. The smooth variation of the left arm of the distribution curve clearly indicates that the employed grid-size resolution sufficiently captures the secondary breakup of droplets.

The combined data of trajectory and drop-size distribution forms a vital part of the characterization of the liquid jets in cross flow.

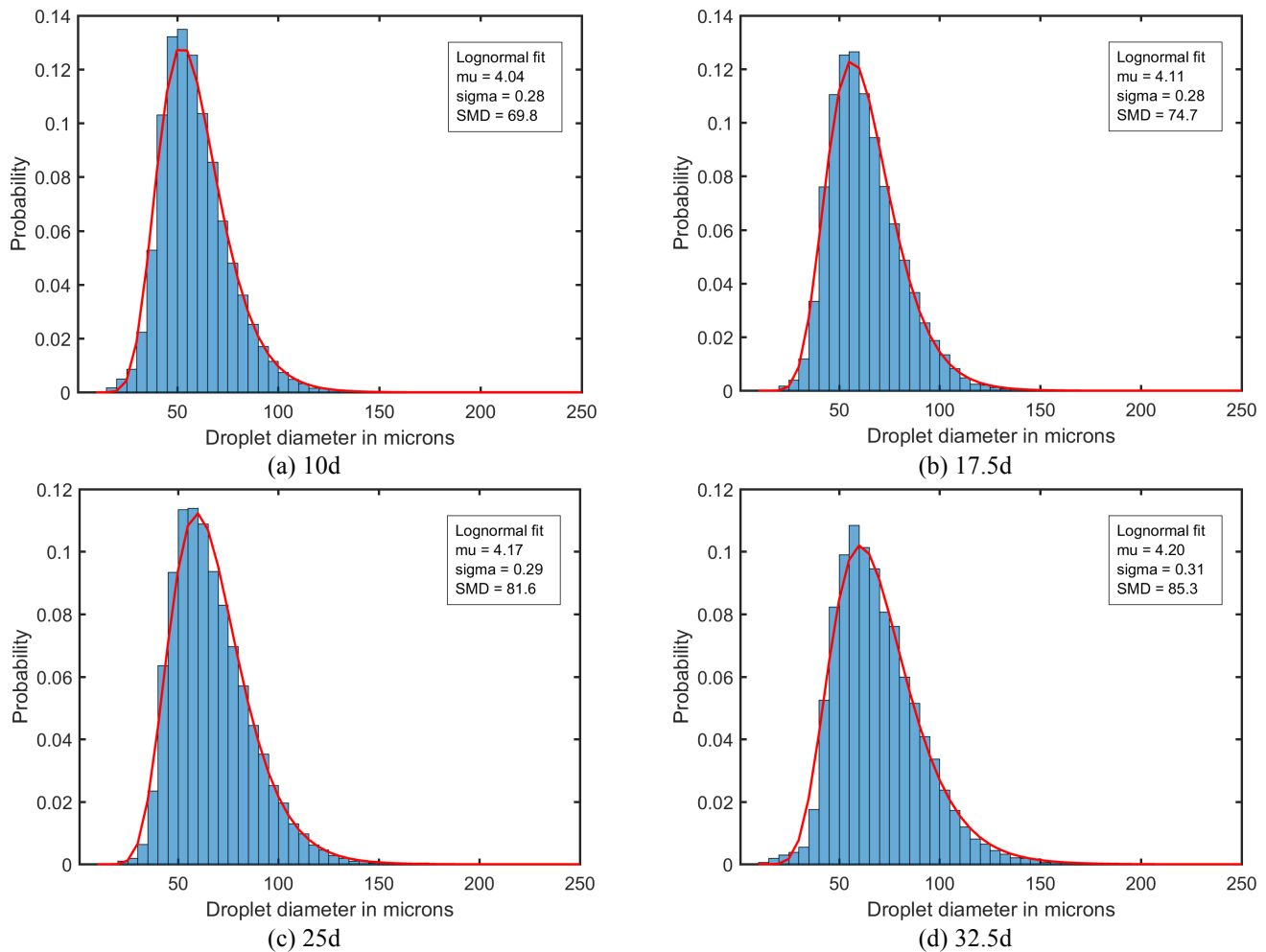


Fig. 7 Drop size distribution and Sauter Mean Diameters (SMD) for $Q=20$, $SN=0$ case at various downstream locations. It is found that the drop size variation is negligible after crossing the $33d$ mark

Table 2. Summary of drop-sizing SMD results

SMD	10d	18d	25d	33d
Q20SN0	69.8	74.7	81.6	85.3
Q20SN4	73.1	78.9	83.4	86.5
Q20SN8	75.2	79.4	89.1	90.8

IV. CONCLUSION

The configuration of liquid jets in a cross flow with swirl has been numerically investigated in the present study. An open source two-phase flow solver Gerris has been used for this purpose. The interface between the solid-liquid phase is tracked with the help of Volume-of-fluid (VOF) advection scheme. The jet with a density ratio (D) of 180:1 is injected radially outwards from the inner tube of the annular computational domain. The simulations are conducted at liquid-to-gas momentum ratio (Q) 20 and 25 for a non-

swirling case and swirling cases with Swirl numbers (SN) 0.42 and 0.84. The liquid jet breakup manifests breakup features very similar to those observed in experimental studies – column breakup, shear breakup and bag-like structures. The instabilities on the windward side of the liquid jet are also clearly observed which require further analyses to quantify the data. Swirling component of the gas flow is found to cause angular deflection of the resultant spray expectedly in the direction of swirl flow itself. Thus, the trajectory of the resultant spray, which is 3-dimensional in nature, is analysed and a correlation for the same is derived in terms of radial penetration and angular deflection. Radial penetration part of the trajectory correlations is able to match those derived from

the experimental observations both in form and magnitudes. Angular deflection of the spray is found to vary linearly with axial distance and also proportional to the corresponding Swirl Numbers (SN). The spray formed as a consequence of primary and secondary atomization is analysed for drop size distribution and it is found that they closely follow the Lognormal distribution. It is also observed that the SMD of the spray follows an increasing trend as we move along the spray in the streamwise direction. This is primarily attributed to the coalescence of droplets. The results obtained in the current investigation are encouraging enough to pursue and extend the study the phenomena in greater detail in the future.

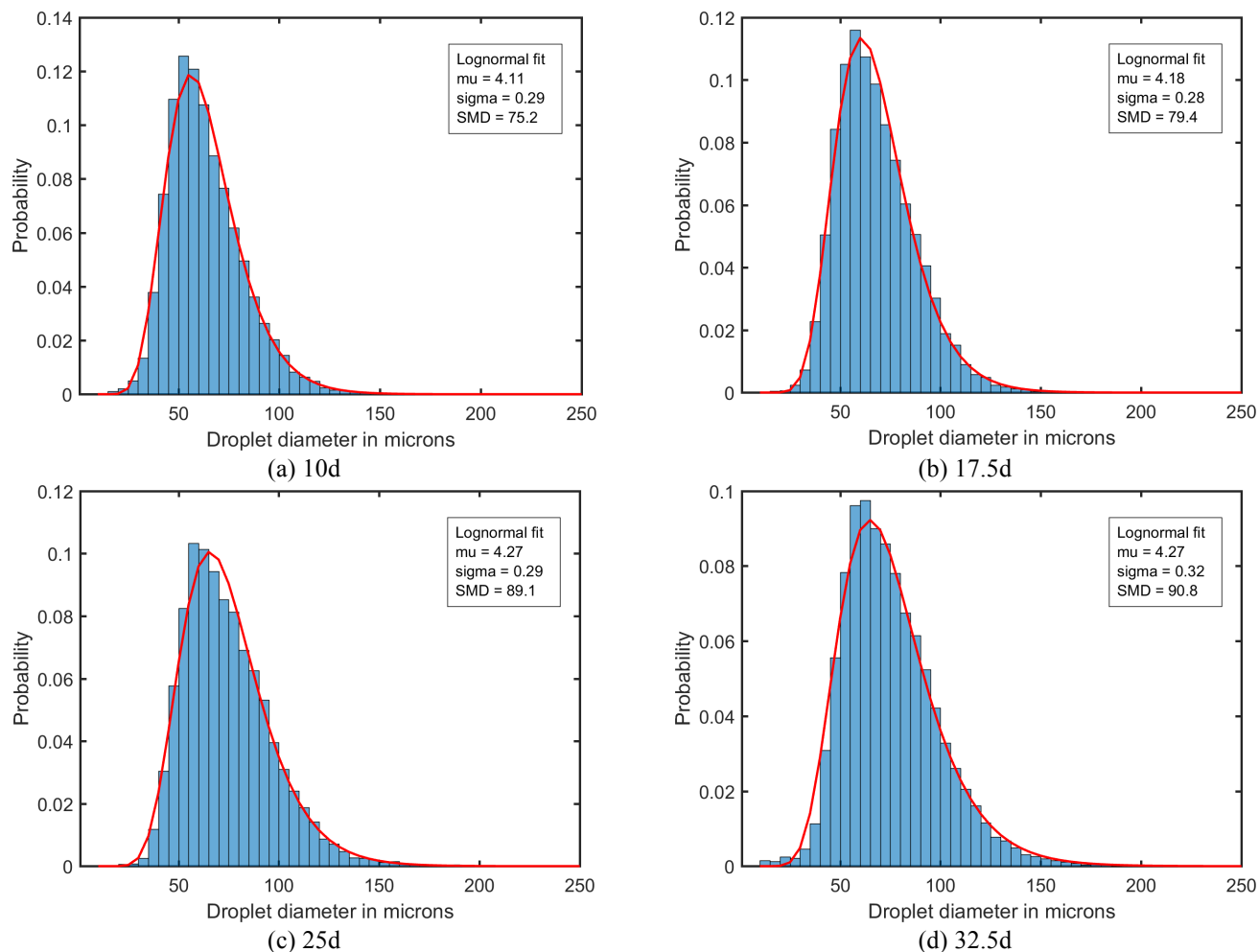


Fig. 8 Drop size distribution and Sauter Mean Diameters (SMD) for $Q=20$, $SN=0.84$ case at various downstream locations. It is found that the drop size variation is negligible after crossing the $33d$ mark

ACKNOWLEDGMENT

The authors would like to thank Pratt and Whitney for the support rendered during the current numerical investigation.

REFERENCES

- [1] Surya Prakash, R., Liquid jets in crossflow, M.Sc. Thesis, Indian Institute of Science, Bangalore, March. (2012).
- [2] Wu, P. K., Kirkendall, K. A., Fuller, R. P., and Nejad, A. S., Journal of Propulsion and Power, 13(1), pp. 64–72, (1997).
- [3] Wu, P. K., Kirkendall, K. A., Fuller, R. P., and Nejad, A. S., Journal of Propulsion and Power, 14(2), pp. 173–181, (1998).
- [4] Hirt, C. W., and Nichols, B. D., Journal of Computational Physics, 39 (1), p. 201225, (1981).
- [5] Sethian, J. A., Fluid Mechanics, Computer Vision, and Materials Science. Cambridge University Press, (1999).
- [6] Tryggvason, G., Bunner, B., Esmaeeli, A., Juric, D., Al-Rawahi, N., Tauber, W., Hanc, J., Nase, S., and Janc, Y.-J.,

- Journal of Computational Physics, 169(2), pp. 708–759, (2001).
- [7] Tomar, G., Fuster, D., Zaleski, S., and Popinet, S., *Computers and Fluids*, 39, pp. 1864–1874, (2010).
 - [8] Herrmann, M., *Journal of Computational Physics*, 229(3), pp. 745–59, (2010).
 - [9] Kim, D., Herrmann, M., and Moin, P., Vol. 010 of 59th Annual meeting of the APS division of fluid dynamics, American Physical Society. 2006.
 - [10] Herrmann, M., *Journal of Computational Physics*, 227, pp. 2674–2706, (2006).
 - [11] Herrmann, M., ed., 22nd Annual Conference on Liquid Atomization and Spray Systems, ILASS-Americas, (2010)
 - [12] Kataoka, I., *International Journal of Multiphase Flow*, 12(5), pp. 745–58, (1986).
 - [13] Clement, E., and Magnaudet, J., *Physics of Fluids*, 18(103304), (2006)
 - [14] Maxey, M. R., Chang, E. J., and Wang, L. P., *Applied Mechanics Reviews*, 47, pp. 70–4, (1994).
 - [15] Popinet, S., *Journal of Computational Physics*, 190, pp. 572–600, (2003).
 - [16] Popinet, S., *Journal of Computational Physics*, 228, pp. 5838–68, (2009).
 - [17] Fuster, D., Bague, A., Boeck, T., Moyne, L., Leboissetier, A., and Popinet, S., *International Journal of Multiphase Flow*, 35, pp. 550–65, (2009).
 - [18] Puckett, E. G., Almgren, A. S., Bell, J. B., Marcus, D. L., and Rider, W. J., *Journal of Computational Physics*, 130, pp. 269–82, (1997).
 - [19] Francois, M. M., Cummins, S. J., Dendy, E. D., Kothe, D. B., Sicilian, J. M., and Williams, M. W., *Journal of Computational Physics*, 213, pp. 141–73, (2006).